

GYROLIS: Post-processing of vehicle localization software via GPS-gyrometer-odometer coupling

David BÉTAILLE*

LCPC-MI, Centre de Nantes, France

■ ABSTRACT

The GYROLIS software application has been developed through LCPC research efforts in the fields of robotics and localization. By use of Kalman filtering and smoothing, this application outputs the geographic coordinates (i.e. latitude and longitude) of a vehicle equipped with a GPS receiver, a gyrometer and an odometer, along with the associated level of precision. The localization sensors used for estimation purposes (in this case, the gyrometer and odometer) compensate for the lack of GPS availability when traversing masking zones. GYROLIS is employed during the post-processing phase, on the basis of data acquired in real time on the instrumented vehicle. This article shows, for two gyrometers of different categories (fiber-optic KVH RD 2100 and micro-electro-mechanical MicroStrain 3DMG), that the real-time localization error (ranging between a few meters and several tens of meters per minute without GPS, depending on the sensor) is divided by 1.5 (for KVH) and 3 (for 3DMG) by means of smoothing. Results are derived from the linearized Rauch-Tung-Striebel algorithm. This software, which draws its originality by not being strictly specialized in GPS calculations nor dedicated to any single type of equipment, is intended for the sector of geomatics with a focus on applications in urban environments. Following the vehicle localization calculation, this package allows identifying the ultimate geo-referencing of road data and images collected by systems onboard this same vehicle.

GYROLIS : Logiciel de localisation de véhicule en post-traitement par couplage GPS – gyromètre – odomètre

■ RÉSUMÉ

Le logiciel GYROLIS est un produit de la recherche au LCPC dans les domaines de la robotique et de la localisation. Il fournit, par filtrage de Kalman et lissage, les coordonnées géographiques (latitude et longitude) d'un véhicule équipé d'un récepteur GPS, d'un gyromètre et d'un odomètre, ainsi que la précision associée. Les capteurs de localisation à l'estime (ici le gyromètre et l'odomètre) pallient l'indisponibilité du GPS en zone de masquage. GYROLIS s'utilise en post-traitement, à partir de données acquises en temps réel sur le véhicule instrumenté. L'article montre, pour deux gyromètres de classe différente (gyromètres à fibre optique KVH RD 2100 et micro-électro-mécanique MicroStrain 3DMG), que l'erreur de localisation en temps réel (de quelques mètres à quelques dizaines de mètres par minute sans GPS selon le capteur) est divisée par 1,5 (pour le KVH) et 3 (pour le 3DMG) par lissage. Les résultats sont fondés sur l'algorithme de Rauch-Tung-Striebel linéarisé. Ce logiciel, original car non spécialisé en calcul GPS ni dédié à un matériel particulier, s'adresse au secteur de la géomatique et particulièrement ses applications en milieu urbain. Il peut permettre, après calcul de la localisation du véhicule, de géoréférencer au final des données routières et des images collectées par des systèmes embarqués sur ce même véhicule.

* CORRESPONDING AUTHOR

David BÉTAILLE

david.betaille@lcpc.fr

INTRODUCTION AND STATE OF THE ART

Many cities, metropolitan areas and regional authorities have implemented road databases and photo libraries, fed from data and images collected automatically by a fleet of specialized vehicles. GPS is the key system within the geo-referencing process for such vehicles (and hence acts to coordinate all data and image collection), but its limitations are well known within complex environments that cause the satellite masking so familiar to cities in particular. Other sensors, known as estimation sensors (e.g. odometer, gyrometer), prove necessary in assisting with the satellite positioning process. The system can thus be described as hybrid localization, based on a data fusion algorithm.

The fusion step within GYROLIS relies on Kalman filtering with the ability to discard outliers in GPS solutions. This set-up is very standard and constitutes the theoretical basis of many algorithms implemented within real-time navigation systems for automobile applications [1, 2]. GYROLIS processes data that need to be compliant with a certain number of specifications. In terms of sensors however, the software has an open architecture: it offers the possibility to adjust Kalman filter parameters to any type of vehicle instrumentation, as long as the vehicle is equipped with a GPS receiver (whether differential or not), a gyrometer (vertical rotation rate measurement, i.e. for the heading, at a minimum frequency of 10 Hz) and an odometer (measurement of distance traveled).

Yet GYROLIS is also able to operate on a delayed time scale (and no longer just in real time), thus making it possible to significantly improve vehicle localization by smoothing the calculated trajectories in terms of processing data in both the clockwise and counterclockwise directions, i.e. by considering not just past measurements but future measurements as well. The algorithm typically applied within the Bayesian context goes by the name of Rauch-Tung-Striebel (RTS) smoother, for which a description is available in [3, 4]; its application is observed to be optimal for linear systems.

In the data fusion mode for localization, the RTS algorithm is employed for the coupling of inertial measurement units (IMU) with GPS, given that the space state is not composed directly of the position to be estimated, but rather of the difference with the actual position; this difference follows a linear evolution model [5, 6]. It is proposed herein to make use of a system state in position (and heading) whose observation is performed directly by GPS (after projection), yet whose evolution is not linear. This article therefore will demonstrate implementation of an extended Rauch smoother (by analogy with the extended Kalman filter), which enables via first-order linearization to take the vehicle evolution model into account. The theoretical elements that serve to justify this approximation can be consulted in [7].

GYROLIS displays originality to the extent that data fusion for localization is mainly commercially available for real-time applications. Moreover, the supply for trajectory post-process concerns either the kinematic GPS calculation on its own, to the exclusion of all other sensors (e.g. Grafnav, GNSS Solutions, Trimble Total Control, Ski Pro), or complete inertial units (i.e. equipping all 3 axes), whose cost exceeds by an order of magnitude (or even more) the cost of a single vertical gyrometer (a solution that proves satisfactory for many land navigation applications). This software supply, which remains highly limited, is available at Ixsea (*loose* coupling of inertial navigation and GPS positions) and at Applanix and Novatel (*tight* coupling of inertial navigation and distances measured between the GPS receiver and satellites), with a certain level of specialization in fusion software programs utilizing specific equipment. GYROLIS is an open-architecture application from a sensor perspective. It fuses in 2D and therefore does not take full advantage of the most advanced 3D inertial units (which, when run using their dedicated software, are able to keep errors to less than a meter, while GYROLIS with just a single gyrometer, no matter how excellent it may be, reaches 1-meter errors). Moreover, GYROLIS is distributed free of charge.

SENSORS TO BE FUSED

GYROLIS fuses data stemming from both proprioceptive sensors (odometer and gyrometer) and exteroceptive (GPS) sensors.

■ GPS (differential)

Satellite positioning naturally seems appropriate for furnishing vehicle geographic coordinates and for subsequent use in geographic information systems (GIS). Its precision currently stands at a few meters (with the SA, for *Selective Availability*, being deactivated). A submetric precision over large ranges of several hundred kilometers can be obtained in differential GPS mode thanks to paid correction services distributed by geostationary satellite, such as Omnistar in Europe and, more recently, via Egnos, which is the free GPS extension service in Europe. As regards GPS, the interested French-speaking reader is invited to consult [8], which illustrates the benefit of the differential corrections in terms of precision and whiteness on solution time series examples. The atmospheric delay on GPS measurements affects position error most significantly, and these are well modeled in DGPS. The potential for multiple signal trajectories remains (especially for urban settings), and these would naturally exert an influence on the residual error, yet somewhat transiently with respect to dynamic positioning: a test on outliers is run in GYROLIS so as to discard such solutions.

As for the experiments presented in this article, a TRIMBLE Ag132 receiver was mounted on test vehicles (single-frequency receiver L1) operating in DGPS, at 1 Hz.

Unfortunately, GPS cannot provide continuous vehicle positioning. Satellite masking is fairly frequent, with signal deterioration or cutoff, especially in awkward settings such as cities or the forest, and the availability of a navigation solution requires the visibility of 4 satellites (the receiver time offset with respect to Universal Time gets added to the 3 position unknowns). Estimation localization sensors are apparently necessary as a complement to GPS, in that they compensate for any GPS masking. The two types of additional sensors adapted to GYROLIS as input are the odometer and the (heading) gyrometer.

■ Odometer

The vehicle is thus assumed equipped with an odometric device, which could for example be an electromechanical encoder. Its calibration proceeds for example by GPS PPK (*Post-Processed Kinematic*) in static mode between two stations located along an extended straight line (typically 1 km). It is estimated that calibration uncertainty equals 1 “encoder” step over the distance traveled, in assuming that:

- wheels do not slide;
- the road surface is perfectly planar;
- GPS PPK produces a negligible positioning error.

For odometric steps of a few tens of centimeters depending on the vehicles, an error on the traveled distance measurement amounts to less than 1%.

The full potential of estimating the odometric step online is to be underscored, i.e. as part of the filtering process presented further below, along with the position and heading calculation. With onboard sensors, it is easy to prove identification of the encoder step, in conjunction with that of the position and heading, under the sole condition that the vehicle is not idle [9]. Nonetheless, a compromise is introduced between the capacity of the process to identify both a variation (quite improbable) in the encoder step and the precision in calculated positions and headings. After analysis, it was decided to fix the encoder step, since it was considered to be predetermined.

■ Gyrometer (heading)

A large number of gyroscopes are available (often coupled with accelerometers in inertial units). Two technologies form the basis of these instruments: fiber optics (FOG: fiber-optic gyro) and *micro-electro-mechanics* (MEMS). In sum, FOG applies the well-known Sagnac optical effect, while MEMS concentrates on the piezoelectric effect of quartz.

In order to illustrate these remarks, the paper will now present results obtained for the two gyroscopes associated with the two technologies. The test vehicles were thus equipped with either a fiber-optic gyroscope (KVH RD 2100) that delivers the vertical rotation rate at a frequency of 10 Hz or a MEMS unit (MicroStrain 3DMG at 76 Hz) used just for its vertical axis. The heading is obtained by means of integrating the measured vertical rotation rate.

Table 1 lists the main set of characteristics for the gyroscopes used.

It may be considered that the gyro measurement error contains a known bias that has been well corrected in temperature for KVH, yet which for 3DMG remains poorly known and partially dependent upon temperature (with a portion remaining random). Added to this bias is a noise assumed to be white and whose integration yields what is commonly referred to as random walk of the sensor: the noise shifts the angle within an envelope that evolves with the square root of time after integration.

Prior to the fusion process, it would be useful to identify bias in order to retain just one purely-stochastic model of the Gaussian white noise type on the sensor noise component. For sensors with variable bias, an online estimation is feasible. The level of noise can also be raised so as to encompass the unknown part of bias.

Table 1
Primary characteristics
of the KVH RD 2100 and
MicroStrain 3DMG
vertical gyroscopes

Sensor	KVH RD 2100	MicroStrain 3DMG
Noise (random operations)	$0.083^\circ \cdot h^{-1/2}$	$3.5^\circ \cdot h^{-1/2}$
Bias instability (at constant temperature) over the short term (1 hour)	insignificant	$0.02^\circ \cdot s^{-1}$ in 1 h
Bias (over the entire range of temperature)	$< 0.4^\circ \cdot s^{-1}$	$< 0.7^\circ \cdot s^{-1}$

THE MODEL AND ALGORITHM EMPLOYED

■ Filtering

GYROLIS is based on a very classical modeling set-up of the vehicle and onboard sensors, with the initial calculation phase drawn from the well-known theory of Bayesian filtering with an extended Kalman filter (EKF). The state vector (denoted X_k at time k of the temporal sampling) contains the position projected into a plane locally tangent to the Earth's surface and the heading, i.e. $X_k = (x_k, y_k, \theta_k)$. It would be possible to add the gyroscope bias and ultimately the odometer step, yet their estimation would adversely affect both the position and heading. The control vector $U_k = (\Delta s_k, \omega_k)$ is composed of the angular velocity and distance traveled; the observation vector $Y_k = (x_{GPS_k}, y_{GP_k})$ can be determined from the GPS navigation solution (which is also projected), when available. Below is a summary of the sequence of filtering stages implemented.

- Evolution (or prediction) stage

$$\begin{aligned}
 x_{k+1|k} &= x_{k|k} + \Delta s_k \cdot \cos(\theta_k + \Delta\theta_k / 2) + v_x \\
 y_{k+1|k} &= y_{k|k} + \Delta s_k \cdot \sin(\theta_k + \Delta\theta_k / 2) + v_y \\
 \theta_{k+1|k} &= \theta_{k|k} + \Delta\theta_k
 \end{aligned}
 \tag{1}$$

where Δs_k represents the variation in distance traveled between two sampling moments, and $\Delta \theta_k$ corresponds to a basic variation in heading over the same time period (T_s). With a gyrometer, which yields rotational speed ω_k , it can be expressed that $\Delta \theta_k = \omega_k \cdot T_s$. These equations are nonlinear. Model noises (v_x and v_y cumulative, the equation in (1) is exact) and control noises (v_{odo} and v_{gyro} , cumulative on Δs_k and ω_k respectively) are assumed to be centered, Gaussian and white, with variance-covariance matrices Q_{mod} and Q_{ctrl} . The extended Kalman filter in fact applies to the equations in (1) linearized around the current state (first-order Taylor development). The *a priori* variance-covariance matrix $P_{k+1|k}$ is then given by:

$$P_{k+1|k} = A_k P_{k|k} A_k^T + B_k Q_{\text{ctrl}} B_k^T + Q_{\text{mod}} \quad (2)$$

where A_k and B_k represent the Jacobian matrices of evolution with respect to the state and control (partial derivatives from Equations (1) with respect to (x_k, y_k, θ_k) on the one hand and with respect to $(\Delta s_k, \omega_k)$ on the other, as calculated in the current state and control at time k).

Note: Should the prediction be by itself (i.e. when no GPS position is available), notations $X_{k+1|k}$ and $P_{k+1|k}$ are replaced by $X_{k+1|k+1}$ and $P_{k+1|k+1}$ in Equations (1) and (2), respectively.

• Observation (or estimation) stage, which is also noisy (noises $v_{x\text{GPS}}$ and $v_{y\text{GPS}}$ on $x\text{GPS}_k$ and $y\text{GPS}_k$, cumulative), with variance-covariance matrix Q_{GPS}

$$X_{k+1|k+1} = X_{k+1|k} + K_{k+1} (Y_{k+1} - H X_{k+1|k}) \quad (3)$$

with $H = \begin{bmatrix} 1 & 0 & 0 \\ 0 & 1 & 0 \end{bmatrix}$ and K_{k+1} the Kalman gain equal to:

$$K_{k+1} = P_{k+1|k} H_{k+1}^T (H_{k+1} P_{k+1|k} H_{k+1}^T + Q_{\text{GPS}})^{-1} \quad (4)$$

The *a posteriori* variance-covariance matrix $P_{k+1|k+1}$ is then given by:

$$P_{k+1|k+1} = (I - K_{k+1} H_{k+1}) P_{k+1|k} \quad (5)$$

The evolution model (which serves in the prediction stage) and GPS observation contain errors: it is considered that both prediction and observation errors are characterized by normal distributions, whose averages are assumed to be zero and whose variances need to be adjusted depending on the rolling/sliding conditions and sensors selected. The whiteness of GPS position estimation error is a commonly-accepted hypothesis, particularly in differential GPS (DGPS) mode. Moreover, it is to be remarked that the evolution model in the 2D (and not 3D) tangent plane constitutes a corrected approximation during the observation stage and is thus considered negligible (except in the case of traveling tens of kilometers without GPS).

■ Smoothing

Upon completion of the Kalman filtering process, which is applicable in real time, GYROLIS offers the possibility of taking advantage of post-processing. The causality is not constraining and the focus lies in smoothing filter outputs. The smoothing phase that follows filtering is thus considerably more original. The smoother is initialized at the last predicted (or estimated) state after applying the Kalman filter $X_{k+1,\text{lis}} = X_{k+1|k+1}$ with the variance-covariance matrix $P_{k+1,\text{lis}} = P_{k+1|k+1}$. The next smooth state is then obtained by adding to the predicted (or estimated) state a correction

proportional to the deviation between the previous smooth state and the corresponding state predicted by the Kalman filter. This gain, for a nonlinear evolution model, once again contains the Jacobian A_k . The smoothing equations can thus be written as follows, in the case of both prediction and estimation:

$$X_{k,lis} = X_{k|k} + C_k (X_{k+1,lis} - X_{k+1|k}) \tag{6}$$

with C_k , the smoothing gain, equal to:

$$C_k = P_{k|k} A_k^T P_{k+1|k}^{-1} \tag{7}$$

The variance-covariance matrix *after smoothing* $P_{k,smooth}$ is then given by:

$$P_{k,lis} = P_{k|k} + C_k (P_{k+1,lis} - P_{k+1|k}) C_k^T \tag{8}$$

In the case of prediction alone, the index notation $_{k+1|k+1}$ replaces $_{k+1|k}$ in Equations (6) through (8).

■ Complete algorithm

The complete algorithm proceeds according to the following stages, with a sampling period of $T_s = 0.1$ s (if necessary, GYROLIS is capable of pre-integrating gyro measurements at a frequency of 10 Hz).

- Calculation of the filtered trajectory: it is observed that 10 predictions lie between two estimations; these give rise to detecting and ultimately discarding possible GPS outliers (a Mahalanobis distance is calculated, and it is then determined for the khi2 law, with a given level of confidence, e.g. 95%, whether this distance is acceptable).
- Calculation of the smoothed trajectory: the same successive prediction and estimation stages are repeated as during filtering.

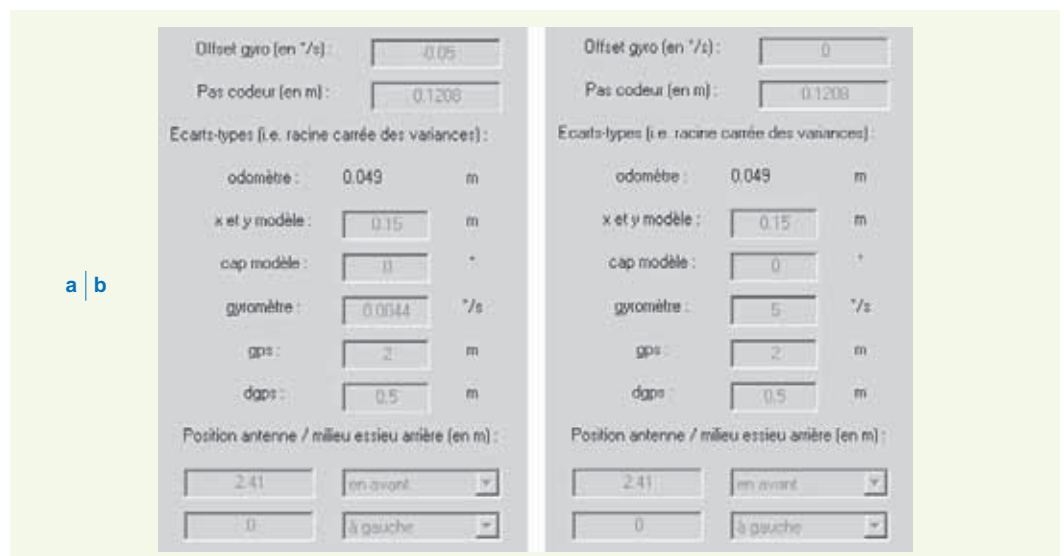
In the end, the filtered and smoothed trajectories are provided, along with estimated precisions.

It is noted that intermediate states $X_{k+1|k}$ and variance-covariance matrices $P_{k+1|k}$, in the presence of both prediction and estimation, are generally not conserved when proceeding with filtering alone; they become necessary to the smoothing step.

RESULTS

GYROLIS was written in Matlab by running the graphic environment in order to open data files, set filtering parameters, display results, etc. In the end, the code was compiled using the *compiler toolbox* and the typically associated C/C++ libraries.

Figure 1
Adjustment parameters for
the two configurations
a: KVH gyrometer
b: 3DMG gyrometer



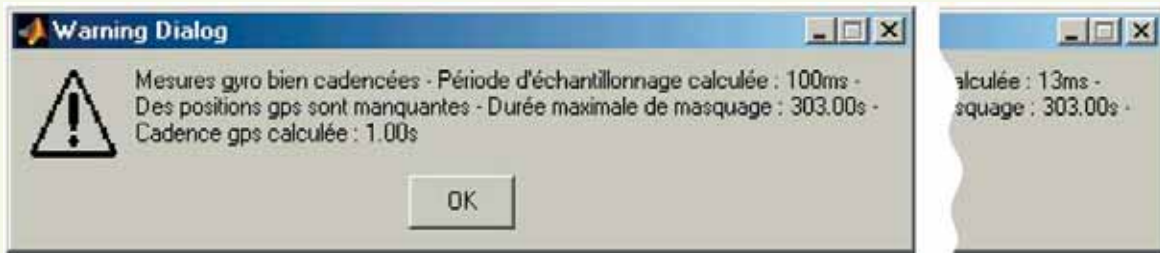


Figure 2

GYROLIS diagnostic of available data for both the KVH (10 Hz) and 3DMG (76 Hz) set-ups

The GYROLIS graphic user interface enables adjusting model, control and measurement noise variances (Figure 1). From a pragmatic standpoint, this adjustment can be carried out by means of a set of tests run on any site where GPS observation conditions are ideal and for which the software simulates satellite masking periods. The adjustment is suitable when predicted errors frame the actual errors. Note that this is indeed validated for the selected sampling, i.e. $T_s = 0.1$ s.

This notion is illustrated based on a test conducted in the city of Rezé using a vehicle equipped with two different types of gyrometers. Adjustments may be performed over the first half of the course (unmasked), while the second half is masked for 5 min (Figure 2).

It is to be pointed out that the standard deviation applied to the odometer is proportional to its step: $\text{pas}/\sqrt{6}$ (this is the standard deviation of a difference in uniform laws); moreover, the model in x and y is characterized by a single standard deviation ($\sigma_x = \sigma_y$), set at 0.15 m (this is the error considered feasible within 0.1 s). For the KVH gyrometer, it is accepted that purely random walk is applicable (Table 1), hence the standard deviation equals this random walk divided by $\sqrt{T_s}$. On the other hand, the standard deviation calculated in this manner is small for 3DMG, whose bias is known to vary, and the adjustment thus involves a test-error process (Figure 3). The GPS is submetric (0.5 m) with the EGNOS differential corrections.

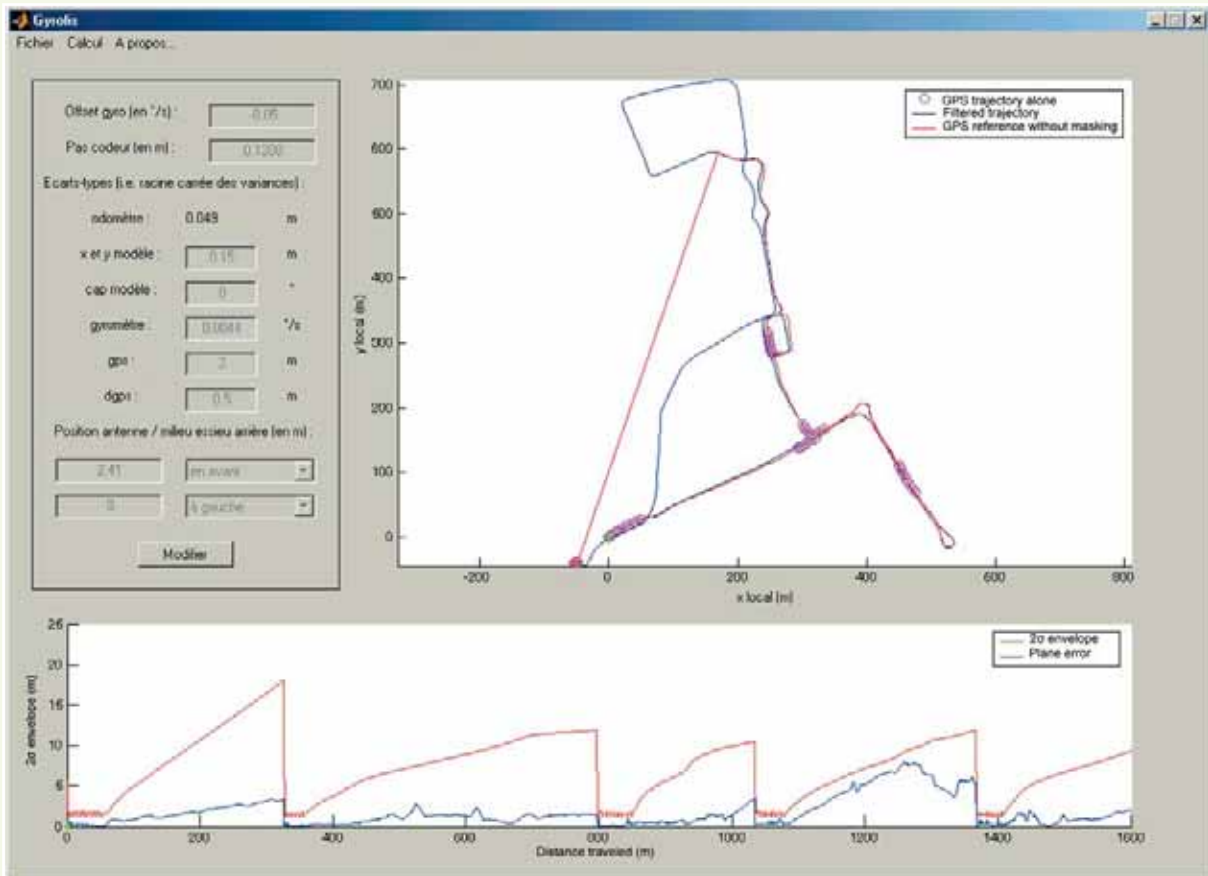
Figures 3a to 6a, 3b to 6b show the following, for the gyrometer configurations KVH and 3DMG respectively:

- filtering with a one-minute mask simulation (in order to adjust parameters);
- smoothing with the same simulation (to be compared with the previous filtering in terms of error);
- then simple filtering (applicable in real time);
- finally smoothing (applicable only in post-processing).

On this series of figures, the upper left-hand corner displays a recall of the parameters used for the current calculation, while the upper right-hand corner presents a plane view of the vehicle trajectory, with the x and y axes (graduated in m) representing the local projection plane tangent to the Earth. The lower figure reveals the predicted error and, for Figures 3 and 4, the true error (in m) along with the traveled distance (in m).

GPS navigation solutions are depicted by magenta circles, while GYROLIS computed trajectories, whether filtered or smoothed, are shown in a solid blue line. The reader is referred to the legend placed in the upper right-hand corner of each figure.

For KVH, the position error increases in $t^{1/2}$ since the angular integration error is small compared to the evolution model error, and the white noise corresponding with this model is integrated once. In contrast, this same error increases in $t^{3/2}$ for 3DMG, which corresponds to a double integration of the gyrometer white noise, predominant in this case.



a
b

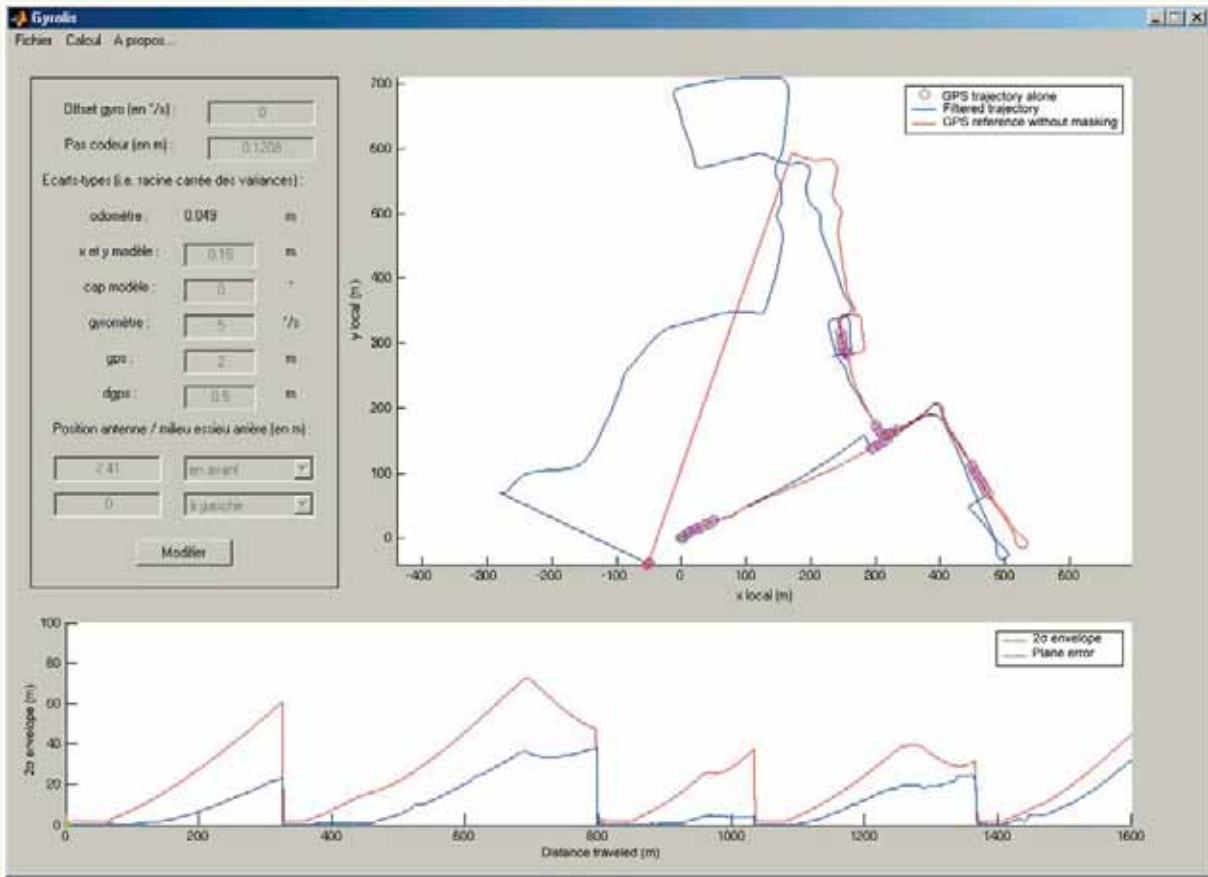
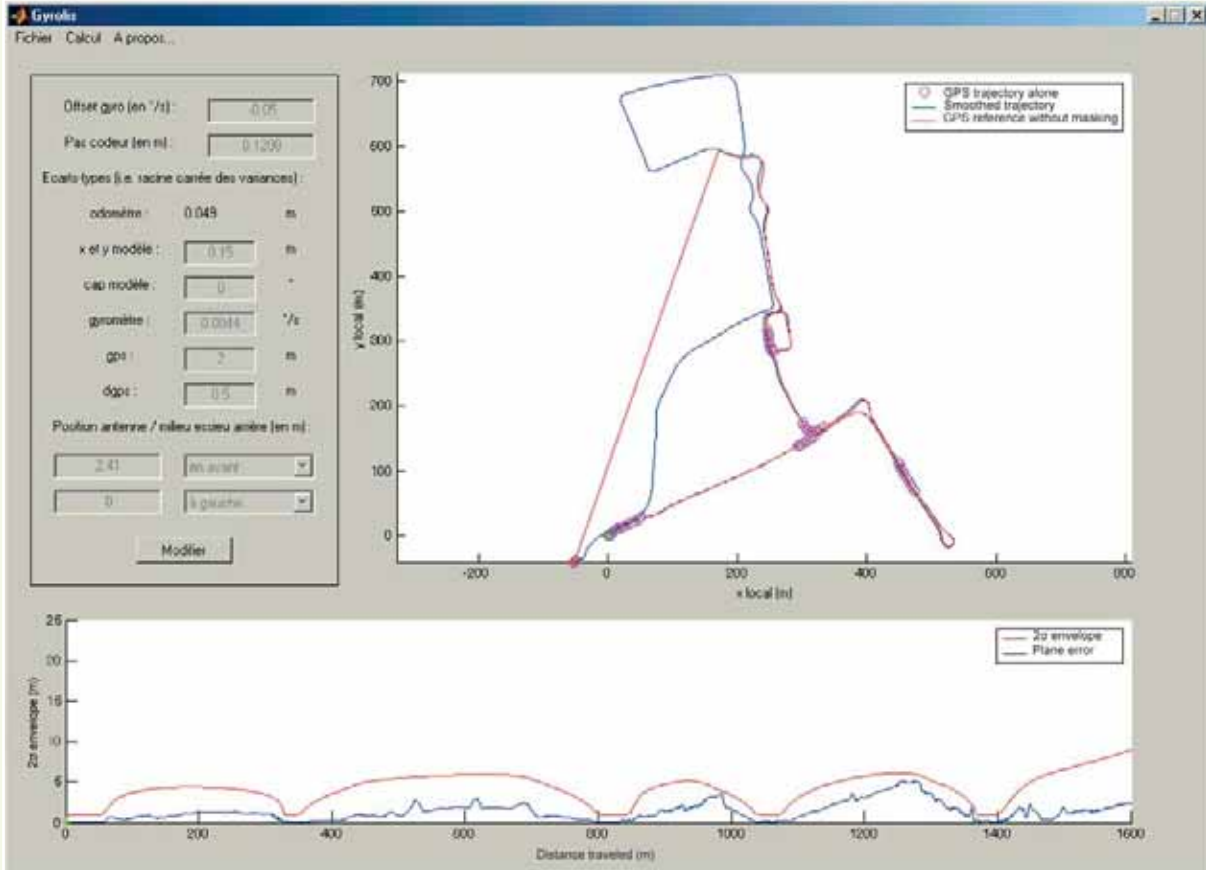


Figure 3

Adjustment with one-minute masking simulation: just the first half of the course can be used, the second half gives rise to an actual 5-minute mask. A close-up is provided of the actual error and the predicted error envelope out to 2 standard deviations (which contains the actual error; thereby validating the adjustment)



a
b

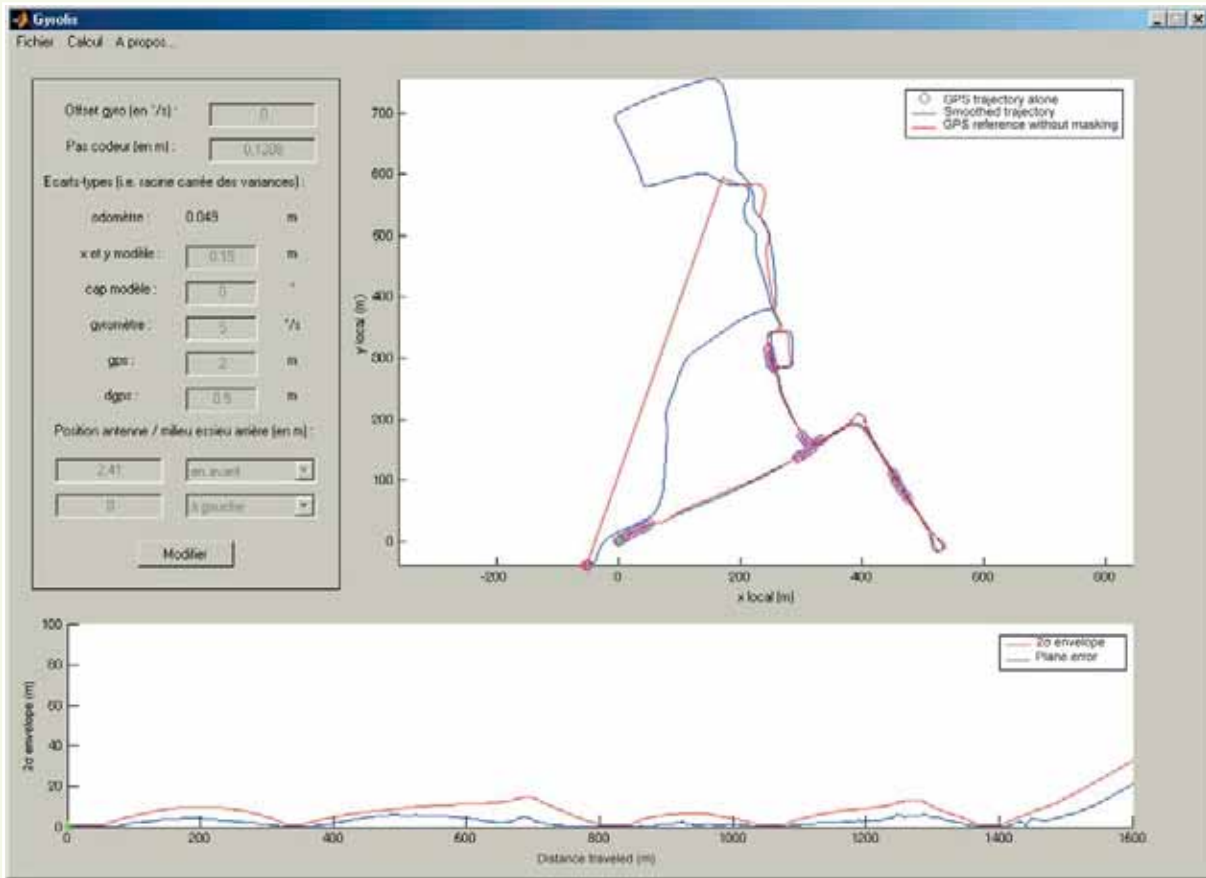
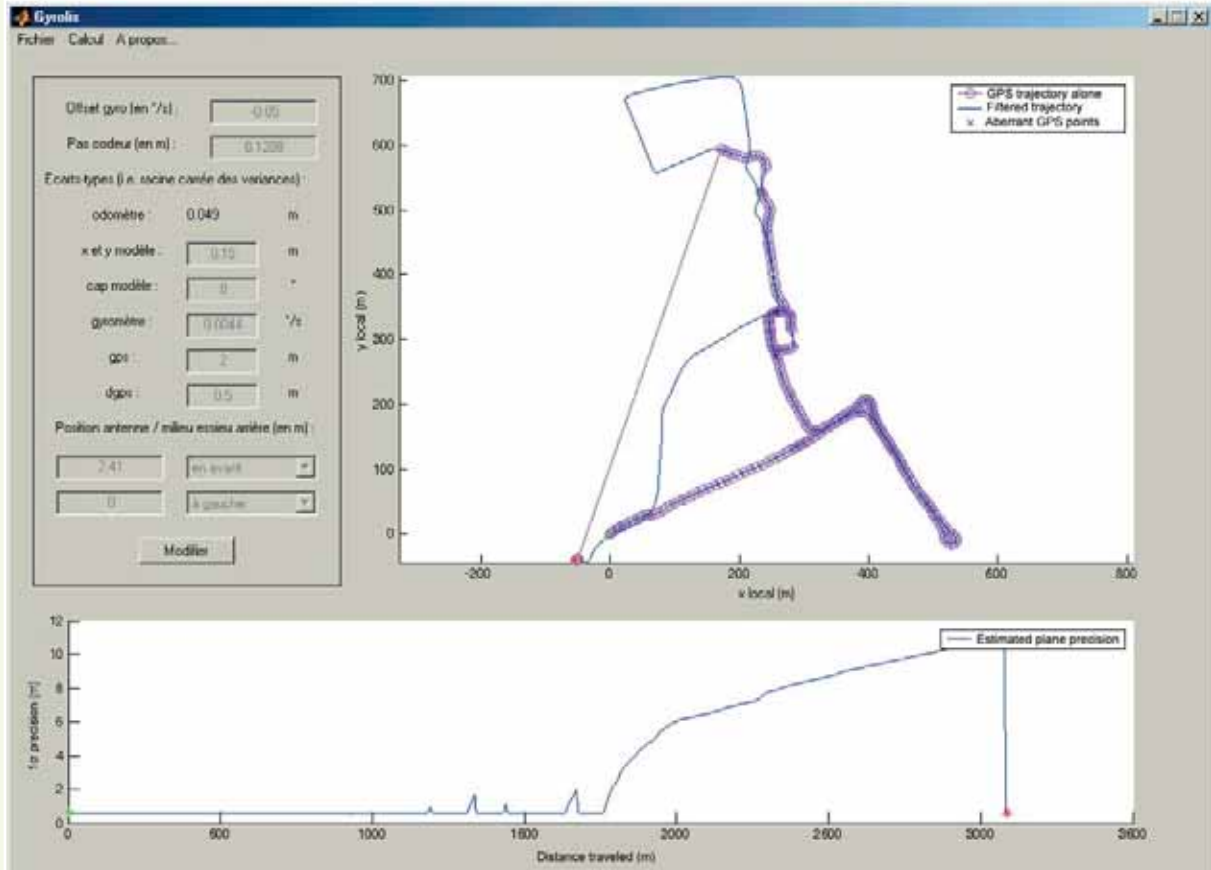


Figure 4

Demonstration of the benefit from smoothing on the same masking series as before (see Fig. 3). The position error increases in $t^{1/2}$ for KVH vs. in $t^{3/2}$ for the 3DMG unit in filtering; in smoothing however, the position error reached lies close to that at mid-mask in filtering, which yields a reduction by a factor of 1.5 and 3, respectively



a
b

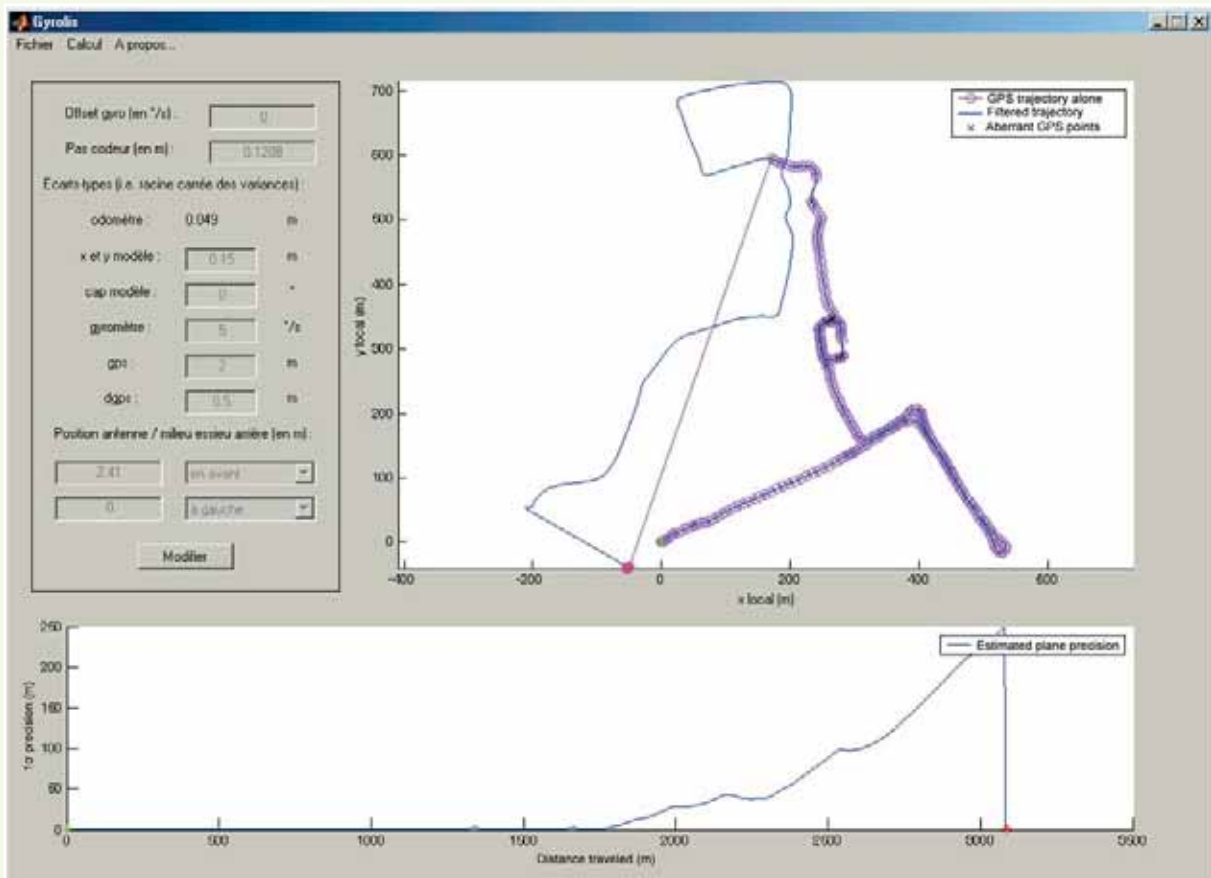
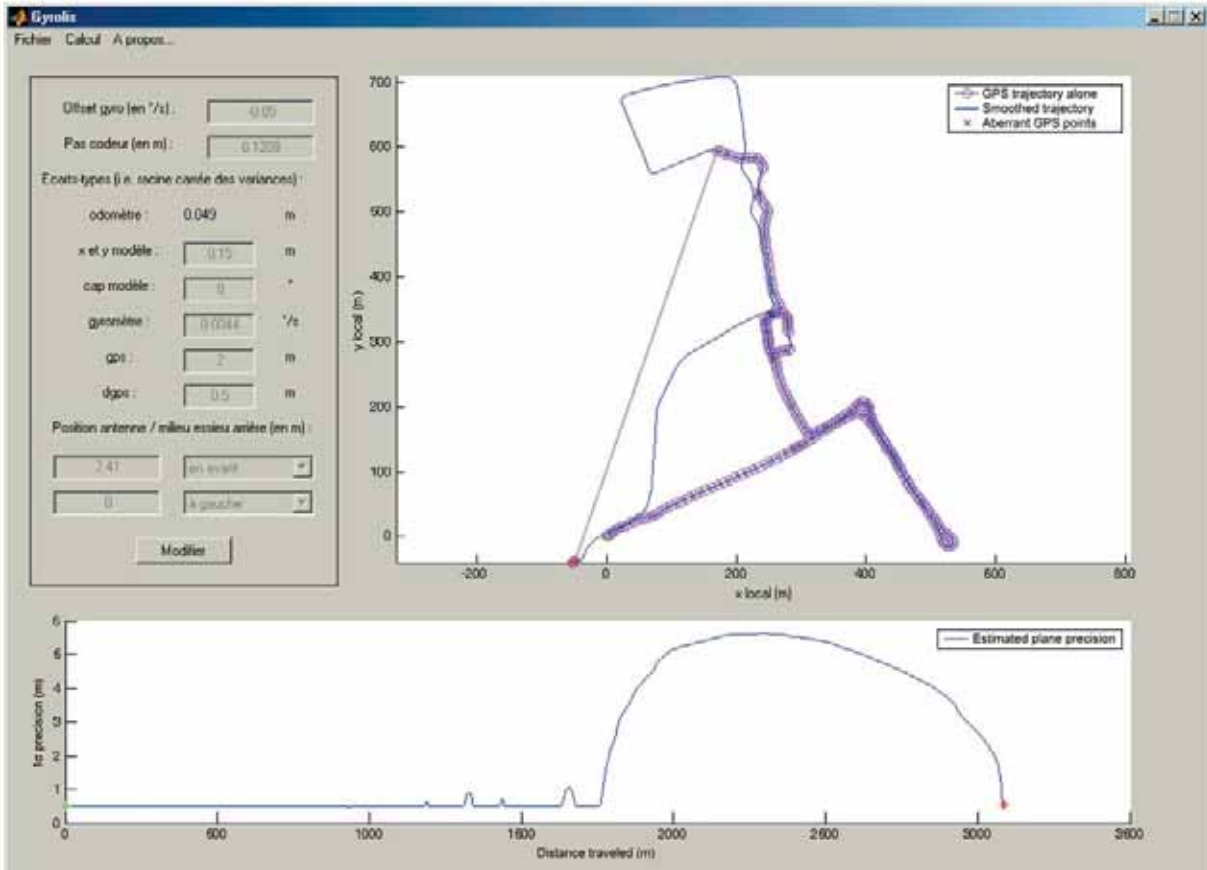


Figure 5

Simple filtering: During the second part of the course, the proprioceptive sensors provide for positioning continuity. The deviation over 5 minutes of the estimated navigation process indicates that the gyrometers appear to be of different categories. Aberrant GPS points are eliminated (see Fig. 7)



a
b

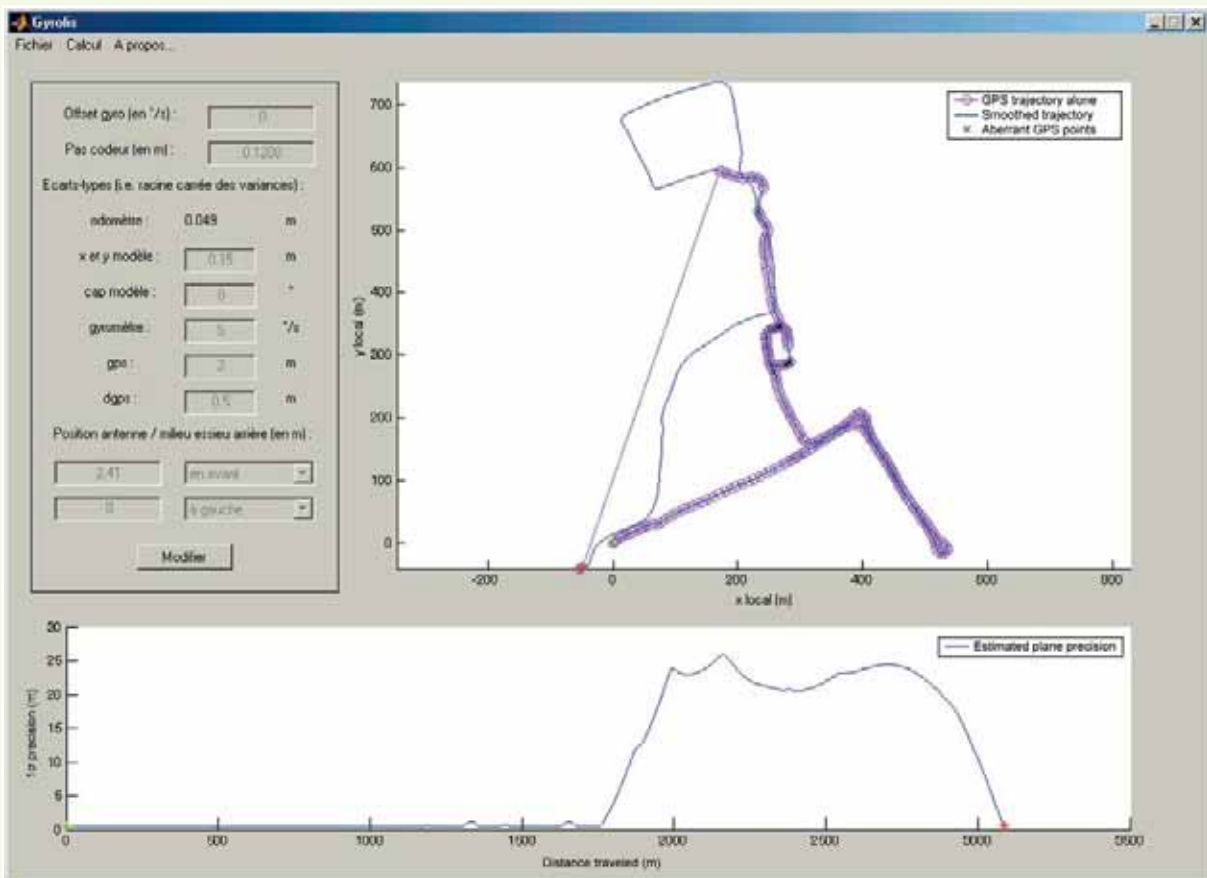
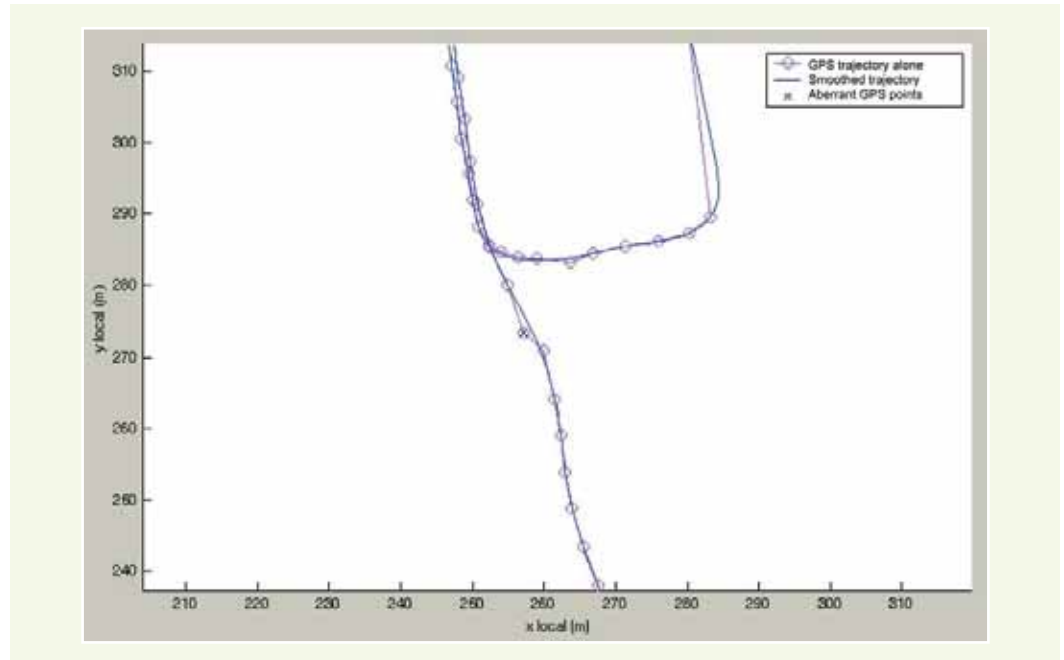


Figure 6

Final smoothing, implementing the complete GYROLIS algorithm: The calculated trajectory using the KVH gyrometer remains precise to within 5 m during the 5-minute mask, vs. 25 m for the trajectory calculated using the 3DMG unit (to 2 standard deviations)

Once the adjustments have been introduced, GPS outliers can be detected during the filtering and smoothing steps; this has been graphically depicted by black crosses. **Figure 7** shows a GPS outlier (thus not used for either filtering or smoothing): such a point can be seen to display a lateral offset as well as an axial offset.

Figure 7
Close-up of **Figure 5a**
in the vicinity of one
aberrant GPS point



Conclusion

This article has presented the results from GPS navigation – dead-reckoning coupling, with the latter being simply composed of the integration of an odometer and gyrometer, under the hypothesis of a locally planar displacement. Kalman filtering, followed by Rauch smoothing, were successively applied to the data. The article reports, for two gyrometers of different categories (a fiberoptic KVH RD 2100 and a micro-electro-mechanical MicroStrain 3DMG), the deviation introduced during GPS masking periods of 1 and 5 min: the order of magnitude for this value is higher for MicroStrain 3DMG (MEMS) when compared with KVH RD 2100 (FOG). For KVH, a plane error that increases in $t^{1/2}$ has been recorded (since the evolution model error is greater than the angular integration error), at an approximate rate of 5 m per minute and 10 m in 5 minutes, whereas it rises more significantly in $t^{3/2}$ for 3DMG. The error envelope for 3DMG corresponds to a white noise (modeling the gyro error) double integration.

The smoothing, which constitutes an extension to the Rauch-Tung-Striebel algorithm over the non-linear domain, enables dividing by 1.5 the deviation obtained during filtering for KVH (or divided by 3 for 3DMG). These findings stem both from the increase in position error in $t^{1/2}$ ($t^{3/2}$ for 3DMG) during filtering and from the smoothing process itself, whose effect serves — as an initial approximation — for halving the time interval between two GPS estimations, and thus for halving the duration of satellite masking. As could be expected, smoothing is not causal and therefore cannot be applied in real time.

REFERENCES

- 1 **BENNETT S.M., ALLEN D.E., ACKER W., KIDWELL R.**, *Blended GPS/DR Position Determination System*, KVH Industries Inc., white paper, **1996**.
- 2 **ABBOTT E., POWELL D.**, Land Vehicle Navigation Using GPS, *Proceedings of the IEEE (Institute of Electrical and Electronics Engineers, Inc.)*, January **1999**, volume **87**, **1**.
- 3 **LABARRÈRE M., KRIEF J.-P., GIMONET B.**, *Le filtrage et ses applications*, 3^e édition, Cépaduès Toulouse, **1993**.
- 4 **BROWN R.G., HWANG P.Y.C.**, *Introduction to Random Signals and Applied Kalman Filtering*, John Wiley and Sons Inc., **1992**.
- 5 **NASSAR S.**, Different Algorithms for Bridging Kinematic DGPS Outages Using SINS/DGPS Integration, *ION GPS*, Oregon, September **2002**.
- 6 **WAEGLI A., SKALOUD J.**, *Assessment of GPS/MEMS-IMU Integration Performance in Ski Racing*, ENC, May **2007**.
- 7 **SIMANDI M., DUNIK J.**, Design of Derivative-Free Smoothers and Predictors, *SYSID*, mars **2006**.
- 8 **DUQUENNE F., BOTTON S., PEYRET F., BÉTAILLE D., WILLIS P.**, *GPS – localisation et navigation par satellites*, 2^e édition, Hermès Lavoisier, **2005**.
- 9 **BONNIFAIT P.**, *Localisation précise en position et attitude des robots mobiles d'extérieur à évolutions lentes*, thèse de Doctorat, université de Nantes, **1997**.

APPENDIX

The GYROLIS software program, developed at LCPC by David Bétaille (along with the contribution from Philippe Bonnifait with the IRCCYN Institute), is the fruit of a research project conducted in the fields of robotics and localization that reached a successful conclusion with its availability online as *freeware* on the LCPC Website in 2007, within favorable context surrounding the interest today in geomatics and especially its potential urban applications. This product is distributed along with a multi-sensor data acquisition software written to run in Windows XP (designed by an engineering student at the Technological University of Compiègne, Vincent Harlé, in 2005), able to directly deliver data compliant with GYROLIS specifications, in guaranteeing accurate data time-stamping (i.e. to within a few milliseconds). When operating in standard configuration, this software offers a specific set of incorporated sensors, containing among other things the gyrometers cited in this article, with the possibility of making additions to this set.

